2020 IEEE/RSJ International Conference on Intelligent Robots and Systems (IROS)
October 25-29, 2020, Las Vegas, NV, USA (Virtual)

Kalman Filter based Range Estimation and Clock Synchronization for Ultra Wide Band Networks

Nushen M. Senevirathna, Oscar De Silva, George K. I. Mann, and Raymond G. Gosine
Faculty of Engineering and Applied Science
Memorial University of Newfoundland

***Abstract*—This paper presents the development of a Kalman filter-based range estimation technique to precisely calculate the inter-node ranges of Ultra Wide Band (UWB) modules. Relative clock tracking filters running between every anchor pair tracks relative clock dynamics while estimating the time of flight as a filter state. Both inbound and outbound message timestamps are used to update the filter to make the time of flight observable in the chosen state space design. A faster relative clock filter convergence has been achieved with the inclusion of the clock offset ratio as a measurement additional to the timestamps. Furthermore, a modified gradient clock synchronization algorithm is used to achieve global clock synchronization throughout the network. A correction term is used in the gradient clock synchronization algorithm to enforce the global clock rate to converge at the average of individual clock rates while achieving asymptotic stability in clock rate error state. Experiments are conducted to evaluate synchronization and ranging accuracy of the proposed range estimation approach.**

I. Introduction

Precise localization in the absence of GPS is a challenging research topic in the area of robotics. During recent years, application of low cost ultra wide band (UWB) ranging devices became significantly popular [1]–[8] mainly due to its small form-factor, simplicity, and availability of higher data rates when compared with other sensor suites in robotics, such as LiDAR, sonar, and visual sensors. One such low cost ranging solution is the DW1000 UWB module by Decawave [9]. These modules can estimate the range between two nodes by measuring the return trip time of a localization message, i.e., two way ranging. The relative clock rate error in internal hardware clock of DWM1000 (typicaly around 5 parts per million (ppm)) scales the measured reply delay and significantly affects the two way ranging accuracy. Therefore, if the clock rate difference can be tracked and corrected accurately, two way range estimation can be significantly improved.

During the past several years a fair number of attempts are reported in the literature to improve two-way ranging accuracy by applying a correction to the clock rate error [10]–[15]. These methods require additional messages to be shared at different stages of the ranging protocol. As an example, asymmetric and symmetric double sided two way ranging methods as discussed in [10], [11], [14], [15] use additional messages after the primary ranging messages. The work shown in [16], [17] have illustrated numerical results for range estimation using the cooperative symmetrical multi-way ranging algorithm while using a simple round robin transmission schedule. Two way ranging is performed twice in this two-phase algorithm to calculate the clock drift. The method is prone to have relatively large ranging errors, mainly due to the large return trip duration in the transmission schedule. Although these discussed methods [10]–[17] have the ability to produce a better range estimation using relative clock rate correction, the noise associated with the transmission and reception timestamps can directly affect the ranging accuracy. Moreover, these methods demand additional power and also can cause interference with other devices when they transmit multiple messages in each ranging cycle. As a hardware solution to measure the relative clock rate, DWM1000 integrates the carrier signal frequency of inbound messages to obtain a direct measurement of the transmitter's clock rate relative to the receiver [4], [18]. However, this measurement too is not suitable to be used as a direct relative clock rate correction due to the significant noise associated as shown in figure 2.

An alternative approach for two way ranging is to make use of a Kalman filter for clock rate estimations. Work in [3] proposes a Kalman filter, and a global clock synchronization algorithm [19] for time difference of arrival based localization. For pairwise synchronization, each Kalman filter takes transmission and reception timestamps of inbound messages as measurements. Return trip time along the transmission schedule is used for time of flight calculation, which is low pass filtered to smooth out remaining noise. This particular low pass filtering approach is intended for self calibration [3] of a stationary set of anchors and is sub-optimal for non-stationary anchors. An improvement can be achieved by estimating the time of flight as a state in the Kalman filter. Thereby allowing the filter to perform tightly coupled estimation of both time of flight and relative clock rates, improving the overall accuracy of two way ranging.

The global clock synchronization step as seen in Kalman filter based clock synchronization methods [3], [19], [20] is an approach used to agree upon a reference clock common

*This work was supported by the Natural Sciences and Engineering Research Council of Canada and Memorial University of Newfoundland.
Authors are with Memorial University of Newfoundland, Canada.
msenevirathna@mun.ca, oscar.desilva@mun.ca, gmann@mun.ca, rgosine@mun.ca

to all nodes in a network. The work carried out in [4] proposes a centralized method to achieve synchronization by considering one anchor's clock as the reference. Network synchronization is achieved by pairwise synchronization with master anchor whose clock is considered absolute. Several other centralized equivalent implementations [5], [8] have used Kalman filters to track the clock dynamics, using timestamps as measurements, where [5] selects master node through a voting scheme. The gradient clock synchronization algorithm which is used in several wireless sensor networks (WSNs) and ranging networks [3], [20], can be considered the state of the art WSN global clock synchronization method, due to its true distributed nature. The main objective of the gradient clock synchronization algorithm as proposed in [19], is to improve the synchronization of nearby anchors. However, it pays less attention to the global clock rate convergence value. Eigenvalue analysis of the error state update matrix as shown in this paper verifies that the scale parameters of the algorithm are only marginally stable. Although the global rate error is shown to be bounded with bounded hardware clock rates, it can scale range measurements of a synchronized network significantly in case of an initialization error or a participation of an inaccurate clock during the initialization. Due to these reasons, it is desirable to seek an algorithm having asymptotically stable properties that can converge the global clock rate to the average of the individual clock rates where the performance is not affected by any unknown or disturbed initial conditions.

This paper presents several novel contributions to improve the UWB range estimation performance while using two way ranging messages. The proposed methodology has incorporated the time of flight as a state in the relative clock tracking filter for accurate estimation of the relative clock dynamics. Accurate modelling of relative clock dynamics allows for more accurate, tightly coupled estimation of time of flight even when anchors are in relative motion. Additionally, the paper proposes a global clock synchronization with a modified update rule which can converge the global clock rate to the average of individual clock rates. The method is superior to the approaches shown in [3] and [19] mainly due to its ability to effectively handle chaotic global clock rate phenomenon. The paper additionally uses carrier frequency integration value as a measurement in the filter for faster convergence of the estimate.

II. Relative Clock Filter

To present the Kalman filter which is used to track the variations of remote clocks, we define two anchors, I, the initiator and J, the responder, considering bidirectional messaging cycle. Each anchor's hardware clock value is considered as a sample of a continuous time process t. Sampled values at transmission (tx) and reception (rx) events of anchor I's clock are represented as $t_I[tx]$ and $t_I[rx]$. To track the smooth variations in relative clock rate, it is sufficient to model the process t as a third order linear system. [3]–[5] The relative rate and acceleration of anchor J's clock with respect to anchor I'c clock at an event ϵ are expressed as,

$$\dot{t}^I_J[\epsilon] = \frac{dt_J}{dt_I}[\epsilon] \tag{1}$$

$$\ddot{t}^I_J[\epsilon] = \frac{d^2t_J}{{dt_I}^2}[\epsilon] \tag{2}$$

As proposed in literature, third derivative of the relative clock phase is considered to be driven by noise [3]–[5].

$$\dddot{t}^I_J[\epsilon] = \frac{d^3t_J}{{dt_I}^3}[\epsilon] = \nu \tag{3}$$

where $\nu(t) \sim N(0, \sigma_c^2)$ is the Gaussian noise driving the system.

A Kalman filter is used to track the relative clock dynamics between remote anchors. Remote anchor J's clock value and its first two derivatives with respect to an anchor I's own clock are chosen to be the filter states. Since time of flight (δ^I_{IJ}) is directly coupled with the estimated clock value, it is also included in the state vector X^I_J.

$$X^I_J = \begin{bmatrix} t^I_J[\epsilon] \\ \dot{t}^I_J[\epsilon] \\ \ddot{t}^I_J[\epsilon] \\ \delta^I_{IJ}[\epsilon] \end{bmatrix} \tag{4}$$

The time of flight (δ^I_{IJ}) is assumed to be noise-driven since no higher derivatives of position or ranges are tracked in this work. Then, the discrete state space system matrix can be found as follows.

$$\Phi = \begin{bmatrix} 1 & dt & \frac{1}{2}dt^2 & 0 \\ 0 & 1 & dt & 0 \\ 0 & 0 & 1 & 0 \\ 0 & 0 & 0 & 1 \end{bmatrix} \tag{5}$$

First three states of the filter can be made observable by taking the inbound timestamps as measurements [3]. Relative clock rate calculated using carrier integration is used as an additional measurement to improve convergence.

Filter measurements acquired by inbound messages are modelled as follows.

$$\begin{bmatrix} y_1 \\ y_2 \end{bmatrix} = \begin{bmatrix} t_J[tx^J_k] \\ \dot{t}^I_J[tx^J_k] \end{bmatrix} \tag{6}$$

Here, the event of transmitting the k^{th} message by anchor J is denoted as tx^J_k and the event of receiving that message by anchor I is denoted as rx^{IJ}_k. Since the system is discretized at the reception event, corresponding output matrix is found as follows.

$$H_1 = \begin{bmatrix} 1 & 0 & 0 & -1 \\ 0 & 1 & 0 & 0 \end{bmatrix} \tag{7}$$

It can be seen that the time of flight is not observable with only one way transmission timestamps. Therefore additional two measurements are obtained using the outbound message reception. Reception timestamp of the outbound messages (y_3) and the clock offset ratio at the reception (y_4) are shared through the next message transmitted by the remote anchor.

$$\begin{bmatrix} y_3 \\ y_4 \end{bmatrix} = \begin{bmatrix} t_J[rx^{JI}_k] \\ \dot{t}^J_I[rx^{JI}_k]^{-1} \end{bmatrix} \tag{8}$$

The system is discretized at the local transmission event and the corresponding output matrix is given below.

$$H_2 = \begin{bmatrix} 1 & 0 & 0 & 1 \\ 0 & 1 & 0 & 0 \end{bmatrix} \tag{9}$$

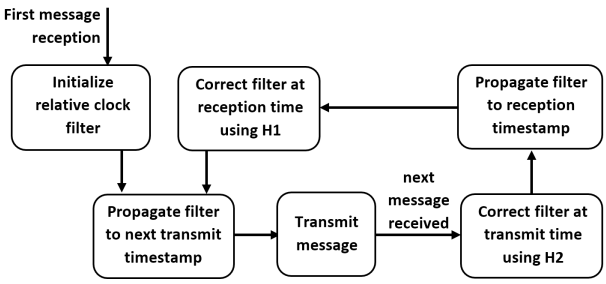

Fig. 1. Filter update flow

Since measurements are only available at local transmission and reception events, the system is propagated and corrected at these events as shown in Fig. 1. Once a transmission time is computed by adding the transmission interval to the previously transmitted timestamp, the states are propagated to the local transmission event before the transmission is performed. When the reply message is received, a correction is applied to the filter with the measurements y_3 and y_4 which are communicated back to node I through the reply message. Then the states are propagated to the local reception event by time interval dt_1^I and they are corrected using y_1 and y_2 measurements.

$$dt_1^I = t_I[rx_k^{IJ}] - t_I[tx_k^I] \tag{10}$$

When the next transmission is scheduled, the states are propagated to the next transmission event tx_{k+1}^I by time interval dt_2^I,

$$dt_2^I = t_I[tx_{k+1}^I] - t_I[rx_k^{IJ}] \tag{11}$$

Standard Kalman filter equations are used to propagate and correct the system. Refer [21] for more information on standard Kalman filter update equations. With filter corrections from measurements, time of flight state is estimated through filter updates.

Although it is desirable to transmit at fixed intervals, DWM1000 discards the least significant 9 bits of the transmission time in delayed transmit mode [18]. Because of this, transmission period cannot be kept constant. Furthermore, there is no guarantee that all the transmitted packets will be successfully received by other anchors. To handle this variation in the sampling time, a time dependent process noise matrix (Q) is defined as suggested in [3].

$$Q = \begin{bmatrix} \frac{\sigma_c^2}{20}dt^5 & \frac{\sigma_c^2}{8}dt^4 & \frac{\sigma_c^2}{6}dt^3 & 0 \\ \frac{\sigma_c^2}{8}dt^4 & \frac{\sigma_c^2}{3}dt^3 & \frac{\sigma_c^2}{2}dt^2 & 0 \\ \frac{\sigma_c^2}{6}dt^3 & \frac{\sigma_c^2}{2}dt^2 & \sigma_c^2\ dt & 0 \\ 0 & 0 & 0 & \sigma_\delta^2 dt \end{bmatrix} \tag{12}$$

Here σ_c^2 is the noise covariance driving the clock dynamics and and σ_δ^2 is the covariance for the time of flight, which depends on the movements of the anchor. It is assumed that there is no correlation between σ_c^2 and σ_δ^2.

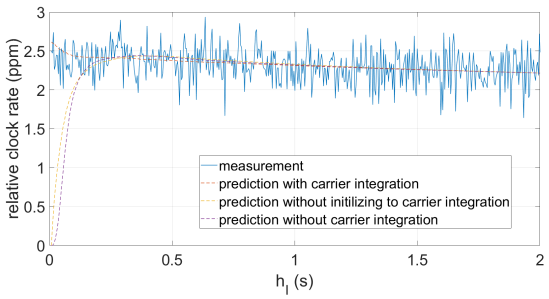

Fig. 2. Relative clock rate convergence comparison

To evaluate the importance of clock offset ratio measurement in the relative clock tracking filter, logged timestamps are used to update filer offline with and without the clock offset ratio measurement. Convergence plots are shown in Fig. 2. For comparison, relative clock rate estimations without initializing to the measured rate is also plotted. It can be seen that the convergence time of tracked relative clock rate has been improved by incorporating the clock offset ratio measurement. Although all estimates converge to the same value within a seconds, this convergence time improvement is significant for low-power applications, where anchors are allowed to sleep between transmissions.

III. Global Clock Synchronization Algorithm

Global clock synchronization algorithm performs the task of converging upon a global reference clock common to all nodes in the network. The relation between each anchor's hardware clock to the global logical clock is expressed as a Taylor series to handle long term variations effectively.

$$l^I(t_I) = t_0^I + d_1^I(t_I - t_0^I) + \frac{1}{2}d_2^I(t_I - t_0^I)^2 + .. \tag{13}$$

where, $l^I(t_I)$ is the global time estimated by anchor I at local time t_I and t_0^I is the global time at the synchronization event. Parameters d_1^I, d_2^I, .. are derivatives of global time with respect to anchor I's clock. The synchronization is achieved by estimating these parameters. During testing it was found that first order approximation is sufficient to track variations between used transmission intervals. Equating the global time at a particular event computed by two nodes and partially differentiating that equation will yield two estimations for t_0^I and d_1^I .

$$\hat{t_0^I} = t_0^J + d_1^J(t_J - t_0^J) - d_1^I(t_I - t_0^I) \tag{14}$$

$$\hat{d_1^I} = d_1^J \frac{\partial t_J}{\partial t_I} \tag{15}$$

The update rule is then established to correct t_0^I and d_1^I based on these estimations. Although the parameterization is slightly different, the method is similar to that in gradient clock synchronization algorithm [3], [19], [20]. The generic gradient clock synchronization update rule is given below which is similar to work in [19].

$$t_{0k+1}^I = t_{0k}^I + \frac{\sum \hat{t_{0k}^I} - t_{0k}^I}{n+1} \tag{16}$$

$$d^I_{1\,k+1} = d^I_{1\,k} + \frac{\sum \hat{d}^I_{1\,k} - d^I_{1\,k}}{n+1} \tag{17}$$

It can be observed that the original gradient clock synchronization method in [19] exhibits chaotic behaviour during clock rate convergence. Although the global rates calculated by each anchor using (17), has shown to be converging, the row stochasticity test used, can guarantee only marginal stability. Since the global clock rate does not have any real tie to the physical clock rates, the global clock rate can be scaled by an arbitrary amount. In order to make the logical clock rate converging to the average rates of individual anchors, a correction term has been added to the proposed update rule of d^I_1. With the assumption that the global clock rate should ideally reflect the average of individual clock rates, another estimate for the d^I_1 parameter is calculated using the constraint in (18), as shown below.

$$\sum (d^I_{1\,k} - 1) = 0 \tag{18}$$

$$\hat{d}^I_{1\,k} = 1 - \sum_{J \neq I} (d^J_{1\,k} - 1) \tag{19}$$

By combining this estimate with a weight K we obtain the following update rule.

$$d^I_{1\,k+1} = d^I_{1\,k} + \frac{\sum (\hat{d^I_1}^J_{\,k} - d^I_{1\,k})}{n+1} + \frac{K}{n+1}\Big(1 - d^I_{1\,k} - \sum_{J \neq I} (d^J_{1\,k} - 1)\Big) \tag{20}$$

It can be seen that the additional term does not change the row sum of the rate parameter update matrix as the term will evaluate to zero for correctly tracked clock rates. Hence, the row stochasticity test for convergence shown in [19] is still valid. An eigenvalue test of the clock error state update matrix resulted unity eigenvalue for the generic update rule and $1-K$ for the novel update rule. By choosing K appropriately, we can drive the error state asymptotically towards zero.

Within the round robin transmission schedule, each anchor updates their individual parameters using the described update rules, before performing a transmission. However, since there is no particular advantage having a global time converging to the average of individual clock values, the above correction term has not been used in the t^I_0 parameter update rule.

Robustness of this update rule against a simulated disturbance was tested on the hardware platform by increasing

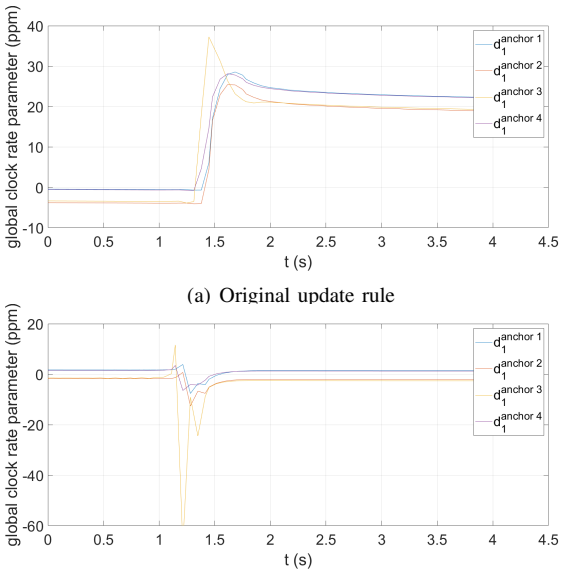

(a) Original update rule

(b) Modified update rule

Fig. 4. Global clock rate parameters

the initial state covariances of the filter in one anchor. When that particular anchor joined the network, global clock rate parameters of all anchors experienced a disturbance. Settlement of these parameters can be seen in Fig. 4(a) and Fig. 4(b). As a result of the marginal stability of the original update rule the global clock rate parameters settle at a higher error resulting a scaling in the global time progression rate. While the modified update rule has the ability to converge the parameters back to the original values within a relatively very short period of time.

IV. Experiments and Results

Real-time tracking performance of the filter was evaluated by logging filter states and measurements for a stationary anchor pair. Noise figures were tuned to achieve a smooth relative clock rate that would correctly track the noisy clock offset ratio measurement. The variation of the filter states with measurements and errors are shown in Fig. 3. When collecting data, the logging anchor (I) was turned on few minutes before the remote anchor (J) to accommodate a cold start.

For comparison, direct calculated time of flight (tof_{DC}), has been plotted with tracked time of flight state in Fig. 3(c). It should be noted that the $\dot{t^I_J}$ value used here is the clock offset ratio calculated using carrier integration. In Fig.

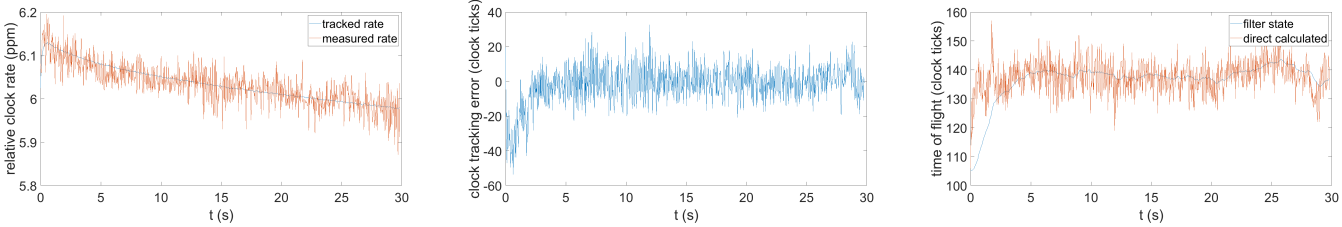

(a) Relative clock rate

(b) Clock tracking measurement error

(c) Time of flight

Fig. 3. Filter performance

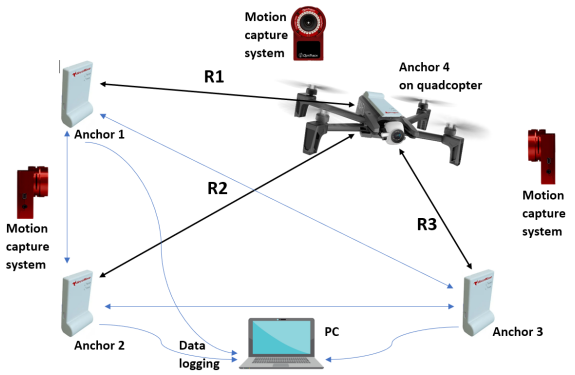

Fig. 6. Experimental setup

3(c), it is apparent that the filter has reduced the range noise efficiently while tracking the low frequency variations.

$$tof_{DC} = \frac{1}{2}((t_I[rx_k^{IJ}] - t_I[tx_{k-1}^I]) - \dot{t_J^I}(t_J[tx_k^J] - t_J[rx_{k-1}^{JI}])). \quad (21)$$

To evaluate the synchronization accuracy and repeatability of the proposed method, anchor network was initialized multiple times and synchronization error was recorded. After 30s from the power-up, data has been collected for a duration of one minute and experiments were conducted keeping about 10 minute down time in between. Here, the synchronization error is calculated as the difference between the global time calculated by two anchors at a local transmission event. It should be noted that the experimental network of this work uses a longer cycle time to accommodate the low power microcontroller. With a faster microcontroller it is possible to achieve a faster cycle time with even less synchronization errors. Standard deviation for all measurements was found to be 2.594 clocks, which translates into a time error of 40ns. This is about 20% better performance as compared to that is presented in [3 Fig.6].

TABLE I
SYNCHRONIZATION ERRORS

Standared deviations (clocks)	σ_{12}	σ_{13}	σ_{14}
test 1	2.258	2.562	2.295
test 2	2.480	3.122	2.646
test 3	2.482	2.659	2.073
test 4	2.439	3.549	2.378
test 5	2.093	2.922	2.052

Performance of range estimation of the filter for a typical robot localization scenario was evaluated by recording the estimated ranges between stationary anchors and a mobile node. As shown in Fig. 6, three stationary anchors were placed at vertices of a 3m by 3m square, and a fourth anchor is attached to a quadcopter which is manually flown along an arbitrary flight path. Ranges calculated by the time of flight state were logged and compared with the ground truth taken from a motion capture system. For comparison, standard two way ranging measurements corrected using tracked relative clock rate, and corrected using carrier integration measurement are also plotted. Since antenna biases are now involved in the range measurements, the fixed bias component has been removed from the logged data. The range error is calculated as the difference between the measured range and ground truth obtained from motion capture system. Root mean square error (RMSE) of the range tracked by the filter turned out to be around 10cm, over range measurements up to 4m. With long return trip durations in a transmission schedule, carrier integration correction alone is insufficient as the RMS errors can be large as 1m. Estimated range data can be used to update a localization filter to track the location. For reference, the path that the quadcopter flew along, captured by the motion capture system is presented

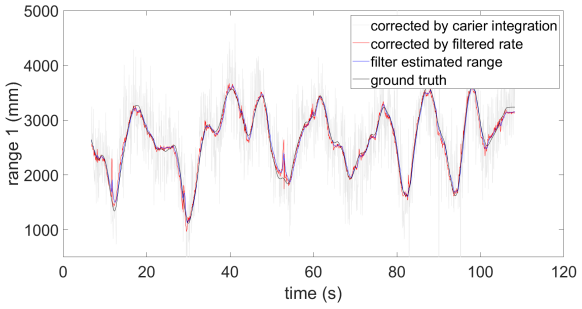

(a) Range 1

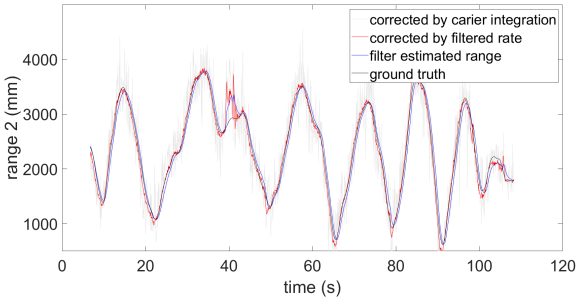

(b) Range 2

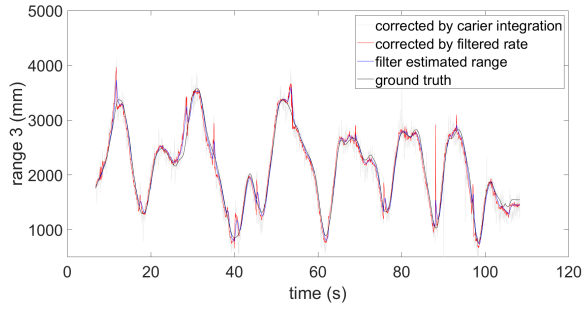

(c) Range 3

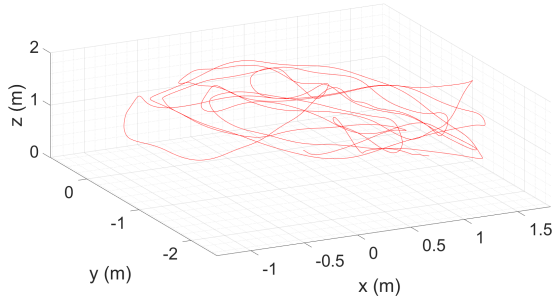

(d) Tag path for the range data-set

Fig. 5. Experiment results

in the Fig. 5(d). Multimedia attachment with this paper illustrates the performance of the proposed method for range estimation in this experiment.

TABLE II
RMS RANGE ERRORS

RMSE (mm)	$R1$	$R2$	$R3$
Kalman filter estimate	68.8	115.8	94.5
Corrected with tracked relative clock rate	106.4	130.6	162.3
Corrected with carrier integration	491.5	1083.5	1358.0

V. CONCLUSION

This paper has presented an improved Kalman filter based method to estimate the time of flight between a set of UWB anchors for range estimation purposes. The time of flight is considered as a state in a Kalman filter which uses transmission and reception timestamps of inbound and outbound messages together with the clock offset ratios calculated using carrier integration at the reception of inbound and outbound messages as measurements. Since ranging is performed while adhering to a transmission schedule, the power consumption for transmission and interference can be kept to a minimum. It is important to note that the added state of the Kalman filter has introduced an additional computational complexity to the algorithm. With the low power microcontroller platform used (MDEK1001 Development kit module by Decawave) in this paper, the implementation has achieved 15ms transmission period for an anchor pair. Since the overhead is mostly on double floating point calculations, a device with a compatible hardware FPU would be able to produce faster and improved updates.

Authors in [3] has stated that they have experienced occasional loss of synchronization due to high packet losses. We, in our experiments, also experienced occasional loss of synchronization when using the original update rule. However, the modified global clock rate parameter update rule used in this paper is able to converge global clock rate parameters to original values even after a temporary disturbance. It guarantees the convergence of the global clock rate at the average of individual clock rates, thus eliminates this chaotic behaviour.

The results indicated that this method can estimate the range between two nodes with a higher precision and accuracy as compared to the traditional two way ranging method. It has the ability to filter out higher frequency noise while capturing low frequency variations efficiently in time of flight calculations. Closely observing the tracked range plots, it could be noted that the resulting RMS errors are mainly due to the lag in the time of flight tracking with fast movements. This can be corrected by adding a derivative of time of flight as a filter state. Ideally, this relative clock tracking filter can be coupled with a localization filter in order to track the dynamics of a moving anchor to obtain predictions over the time of flight state. For further improvements, antenna delays can also be correctly modelled or calibrated to remove the inherent biases in range measurements. A received signal power and orientation based correction for antenna biases may further improve the ranging accuracy as proposed in some literature [18], [22]. Future work will target extending the network to use both difference time of arrival and scheduled ranging methods based on the availability of the anchors, and implement the calibration and localization frameworks for robot localization purposes.

REFERENCES

[1] S. Gezici, Zhi Tian, G. B. Giannakis, H. Kobayashi, A. F. Molisch, H. V. Poor, and Z. Sahinoglu, "Localization via ultra-wideband radios: a look at positioning aspects for future sensor networks," *IEEE Signal Processing Magazine*, vol. 22, no. 4, pp. 70–84, July 2005.

[2] J. González, J.-L. Blanco, C. Galindo, A. Ortiz-de Galisteo, J.-A. Fernández-Madrigal, F. A. Moreno, and J. L. Martinez, "Mobile robot localization based on ultra-wide-band ranging: A particle filter approach," *Robotics and autonomous systems*, vol. 57, no. 5, pp. 496–507, 2009.

[3] M. Hamer and R. D'Andrea, "Self-calibrating ultra-wideband network supporting multi-robot localization," *IEEE Access*, vol. 6.

[4] J. Cano, S. Chidami, and J. Le Ny, "A kalman filter-based algorithm for simultaneous time synchronization and localization in uwb networks," in *2019 International Conference on Robotics and Automation*.

[5] F. Kirsch and M. Vossiek, "Distributed kalman filter for precise and robust clock synchronization in wireless networks," in *2009 IEEE Radio and Wireless Symposium*.

[6] A. Prorok, L. Gonon, and A. Martinoli, "Online model estimation of ultra-wideband tdoa measurements for mobile robot localization," in *2012 IEEE International Conference on Robotics and Automation*.

[7] A. Prorok and A. Martinoli, "Accurate indoor localization with ultra-wideband using spatial models and collaboration," *The International Journal of Robotics Research*, vol. 33, no. 4.

[8] K. Liu and Z. Li, "Adaptive kalman filtering for uwb positioning in following luggage," in *2019 34rd Youth Academic Annual Conference of Chinese Association of Automation (YAC)*.

[9] "Decawave." [Online]. Available: https://www.decawave.com/

[10] Y. Jiang and V. C. Leung, "An asymmetric double sided two-way ranging for crystal offset," in *2007 International Symposium on Signals, Systems and Electronics*.

[11] D. Neirynck, E. Luk, and M. McLaughlin, "An alternative double-sided two-way ranging method," in *2016 13th workshop on positioning, navigation and communications (WPNC)*.

[12] M. Kwak and J. Chong, "A new double two-way ranging algorithm for ranging system," in *2010 2nd IEEE InternationalConference on Network Infrastructure and Digital Content*.

[13] Y. Saigo, S.-i. Ko, J.-y. Takayama, and S. Ohyama, "Precise asynchronous rf tof measurement based on two-way-ranging using heterogeneous clocks," in *2012 Proceedings of SICE Annual Conference (SICE)*. IEEE, 2012, pp. 1437–1442.

[14] B. Al-Qudsi, M. El-Shennawy, N. Joram, and F. Ellinger, "Crystal oscillator frequency offset compensation for accurate fmcw radar ranging," in *2016 German Microwave Conference (GeMiC)*.

[15] H. Kim, "Double-sided two-way ranging algorithm to reduce ranging time," *IEEE Communications letters*, vol. 13, no. 7.

[16] F. C. P. Shin, L. Zhiwei, and L. J. Xing, "Symmetric multi-way ranging for wireless sensor network," in *2007 IEEE 18th International Symposium on Personal, Indoor and Mobile Radio Communications*.

[17] J. Lee, Z. Lin, P. Chin, and C. L. Law, "The use of symmetric multi-way two phase ranging to compensate time drift in wireless sensor network," *IEEE transactions on wireless communications*.

[18] "Dw1000 user manual." [Online]. Available: https://www.decawave.com/dw1000/usermanual/

[19] P. Sommer and R. Wattenhofer, "Gradient clock synchronization in wireless sensor networks," in *2009 International Conference on Information Processing in Sensor Networks*.

[20] A. C. Pinho, D. R. Figueiredo, and F. M. França, "A robust gradient clock synchronization algorithm for wireless sensor networks," in *2012 Fourth International Conference on Communication Systems and Networks (COMSNETS 2012)*.

[21] R. Faragher, "Understanding the basis of the kalman filter via a simple and intuitive derivation [lecture notes]," *IEEE Signal processing magazine*, vol. 29, no. 5.

[22] J. Sidorenko, V. Schatz, N. Scherer-Negenborn, M. Arens, and U. Hugentobler, "Decawave uwb clock drift correction and power self-calibration," *Sensors*, vol. 19, no. 13.